DOE/ER/40861--1

Technical Progress Report

Development of a Thermionic Magnicon Amplifier at 11.4 GHz

Interagency Agreement No. DE-AI-02-94ER40861

Report No. DOE/ER/40861--1

Submitted to: United States Department of Energy

Submitted by: Plasma Physics Division
U. S. Naval Research Laboratory
Washington, DC 20375–55346

Investigators: Dr. Steven H. Gold
Dr. Arne W. Fliflet
Dr. Wallace M. Manheimer

Report Period: 16 May 1994 – 31 December 1995

MASTER

DISTRIBUTION OF THIS DOCUMENT IS UNLIMITED

Outline

I. Executive Summary

This is a progress report on a four–year research program entitled "Development of a Thermionic Magnicon Amplifier at 11.4 GHz," which is under way in the Plasma Physics Division of the Naval Research Laboratory (NRL) under Interagency Agreement DE–AI02–94ER40681. This report covers the period 16 May 1994 through 31 December 1995. The magnicon is an advanced microwave tube with potential application to future high gradient linear accelerators such as TeV colliders. Under this program, NRL plans to build and test a thermionic magnicon amplifier tube powered by a 500 kV, 200 A, 10 Hz modulator with a 1 μsec pulse. However, the experiments that were carried out during the period covered by this report were driven by a single-shot Marx generator, and the electron beam was produced from a graphite plasma cathode.

DISCLAIMER

This report was prepared as an account of work sponsored by an agency of the United States Government. Neither the United States Government nor any agency thereof, nor any of their employees, makes any warranty, express or implied, or assumes any legal liability or responsibility for the accuracy, completeness, or usefulness of any information, apparatus, product, or process disclosed, or represents that its use would not infringe privately owned rights. Reference herein to any specific commercial product, process, or service by trade name, trademark, manufacturer, or otherwise does not necessarily constitute or imply its endorsement, recommendation, or favoring by the United States Government or any agency thereof. The views and opinions of authors expressed herein do not necessarily state or reflect those of the United States Government or any agency thereof.

II. Introduction

The magnicon [1–3] is an advanced "scanning–beam" microwave amplifier tube for use in powering future high gradient linear accelerators, such as the proposed TeV linear collider known as the Next Linear Collider (NLC). The rf source for the NLC must provide a power of 500 MW to 1 GW per tube in a 200 nsec pulse at a frequency in the range of 10–20 GHz. The required power can either be generated directly in 200 nsec pulses, or generated at longer pulse lengths (e.g., 1–2 μsec) and then pulse–compressed. Because the average power required by the NLC is so large, source efficiency is a crucial consideration. The goal of the NRL program is to produce 50 MW at 11.4 GHz in a 1 μsec pulse, using a 500 kV, 200 A electron beam produced from a thermionic electron gun driven by a 10 Hz modulator.

The magnicon is a "scanning beam" analog to a gyroklystron amplifier, and offers the promise of high power tubes that will operate at very high efficiency (>50%) at frequencies of 10 GHz and above. Scanning–beam devices create phase synchronism between the transverse deflection of the beam and the phase of a rotating rf mode, so that the interaction is invariant on the rf time–scale. This phase synchronism, which occurs without requiring a separate bunching mechanism, makes possible very high efficiencies. For example, several gyrocons, which are lower frequency (typically <1 GHz) scanning beam devices, have operated at efficiencies of 80–90% [4]. However, the achievement of high efficiency by means of a scanning–beam interaction also places tight constraints on beam quality.

In order to illustrate the operating principles of the magnicon, a diagram of the NRL magnicon concept is shown in Fig. 1. A magnetized pencil beam from a 500 kV electron gun transits a drive cavity containing a rotating TM_{11} mode generated by an external rf source. The rotating magnetic fields of the TM_{11} mode convert a small fraction of the beam axial momentum into transverse momentum (Larmor motion) about the applied axial magnetic field. The beam then enters a sequence of gain cavities, where the transverse momentum creates rf fields that further

deflect the beam, producing a progressively higher fraction of transverse momentum. This proceeds until the electrons exiting the final deflection cavity, also known as the penultimate cavity, have an $\alpha \geq 1$, where α is the ratio of transverse to parallel momentum. Unlike the gain cavities of the klystron, the gain cavities of the magnicon are not used to create bunching— the electron motion is synchronous with the phase of the rf fields in each of the magnicon cavities, beginning with the drive cavity.

As a result of the phase–synchronous transverse deflection of the electron beam as a whole, the beam electrons entering the output cavity execute Larmor motion *whose entry point and guiding center rotate in space about the cavity axis at the drive frequency.* In the output cavity, the beam transverse momentum is used to drive a cyclotron–resonant fast–wave interaction that extracts principally the transverse beam momentum. This interaction can be highly efficient, because the electrons arrive in the interaction cavity coherently gyrophased. This provides for optimum energy transfer to a mode of the output cavity that rotates synchronously with the deflection cavity modes. However, maintaining a tight phase bunch in the magnicon output cavity requires the use of a good quality, small radius electron beam. The cyclotron resonance extraction mechanism in the magnicon output cavity is analogous to that of a fundamental–harmonic gyrotron, although magnicons typically use TM rather than TE modes. The phase synchronism in the output cavity can take place at either the fundamental or a harmonic of the drive frequency. For an X–band magnicon, it is convenient to operate the output cavity at twice the frequency of the deflection cavities.

The magnicon holds out the promise of a new class of high average power, high efficiency (>50%) microwave amplifier tubes, combining high frequency (>10 GHz) and long pulse (>1 μsec) with frequency and phase stability. However, magnicon technology is significantly less mature than either the klystron or the gyroklystron. A number of critical areas must be addressed in order to demonstrate the magnicon's potential. Among the important issues are: 1) Production of a high–current electron beam with low emittance and energy spread for efficient magnicon

operation, 2) Achievement of α~1 in the deflection cavities, while avoiding rf breakdown, 3) Avoidance of parasitic oscillations, and 4) Optimization of output cavity interaction to achieve η~50%.

III. Cold Cathode Magnicon Experiments

This section discusses the high-power testing of the magnicon amplifier circuit, and summarizes work that is reported in detail in Ref. [5], which is included as Appendix I. The final magnicon design parameters are shown in Table I. The circuit includes a drive cavity, two half–wavelength gain cavities, and a two–section π–mode penultimate cavity, all operating at 5.7 GHz, followed by an output cavity operating at 11.4 GHz. This configuration is shown schematically in Fig. 1. The documentation of this design was completed in Ref. [6].

TABLE I. MAGNICON DESIGN PARAMETERS

Input:	~1 kW @ 5.7 GHz
Beam:	500 keV, 172 A
Deflection cavities:	3 half–wavelength TM_{110}–mode cavities (1 drive, 2 gain) Cavity Radius~3.2 cm; Cavity Length=2.3 cm; Beam Tunnel Radius=0.5 cm; Beam Tunnel Length=1.9 cm
Penultimate cavity:	π–mode two–section TM_{110} cavity, Cavity Radius~3.2 cm, Cavity Length=5 cm
Output cavity:	TM_{210} mode, Q~800 (for 5.5–mm–diam. beam) Radius~2.15 cm; Length=5 cm
Maximum rf fields at walls: (Penultimate and Output Cavities)	~250 kV/cm
Output:	$f_{out} = 4f_{SLAC} = 11.4$ GHz P ~ 20 MW @ η~24% for 5.5–mm–diam. beam P ~ 50 MW @ η~56% for 2–mm–diam. beam Overall gain ~ 44–48 dB

The complete X–band magnicon amplifier circuit completed the final stages of calibration and cold testing, was installed on the Long–Pulse Accelerator facility, and initial hot tests began in late December 1993. In initial tests, 40 dB of gain was observed in the deflection cavities at low drive powers. However, at higher drive powers, a saturation effect was observed, with the maximum deflection cavity powers in the range of 1–10 kW. The causes of this saturation effect were extensively investigated. It was discovered that a cavity "breakdown" process was occurring, typically initiated by the x–ray pulse from the electron beam diode. This breakdown process produces a plasma in the cavities that constitutes a nonlinear cavity load, clamping the level of rf fields in the cavity. The plasma was observed both due to its effect on the cavity loading, and directly by measuring visible light emission from within the cavities.

As a result of these observations, a major effort was made to improve the vacuum conditions. One of the limitations on the achievable vacuum pressure was the very limited vacuum conductance involved in pumping the deflection cavities through the beam pipe. This was improved by pumping the first three deflection cavities from the side through a pair of parallel pumping tubes that connect to the main diode vacuum. In addition, the cavities were disassembled, thoroughly cleaned with detergents and solvents, and then reassembled and put through a low–temperature (~120° C) bakeout. Following this, a new set of measurements was begun.

In initial measurements, the low power saturation effect was still seen during the voltage flat-top under the usual conditions of current and voltage. In order to overcome the plasma loading effect, the experimental parameters were varied in order to greatly increase the rf gain of the deflection cavities. First, the voltage was increased from 500 kV to 650 kV, resulting in a higher beam current. Second, the axial magnetic field (or rather B/γ) was increased. Higher magnetic fields further increase the beam current. As discussed previously, deflection cavity gain increases both with current and with B/γ.

Initial measurements were carried out at 650 kV, 300 A, and 11 kG. Under these conditions, the rf gain process can overcome the low power saturation caused by plasma loading. The result was a short (~50 nsec FWHM) rf gain spike in the penultimate cavity, followed in temporal sequence by gain spikes in the third and second deflection cavities. This temporal sequence is due to the fact that the penultimate cavity has the highest total gain with respect to the drive signal, while the second deflection cavity has the least, and to the fact that the deflection cavity gain is increasing in time due both to the rising current and the falling voltage. The rf in the second, third, and penultimate cavities ramps up to high levels (~80–90 dBm), and then suffers a complete rf breakdown. A small rf signal was observed at the output of the experiment (<100 kW), but its peak preceded the peaks in any of the deflection cavities. These experiments demonstrated that sufficiently high gain could "burn through" the plasma saturation effect. However, at this very high magnetic field, the deflection cavities are not stable, and will ramp up to high power without a drive signal in the first deflection cavity. Also, the small output signal did not correlate well with the timing of the penultimate cavity signal, and was assumed to be a spurious oscillation.

In order to diagnose the output, a new heterodyne diagnostic was constructed to measure the spectrum of the output radiation. This diagnostic combines the output signal with the signal from a tunable local oscillator in a double-balanced mixer, and then acquires the resulting signal using a Tektronix DSA602 digital oscilloscope with an analog bandwidth of ~1 GHz, a 2 GS/s digitizing rate, and an FFT (fast Fourier transform) capability. This diagnostic yields a measurement of $|\Delta f| = |f - f_{LO}| < 1$ GHz to a precision of a few MHz, where f is an emission line from the experiment and f_{LO} is the selected frequency of the local oscillator. By varying the local oscillator frequency on a shot–to–shot basis to remove ambiguities in the sign of Δf, and to rule out signals due to aliasing, spectral features can be determined to a precision of a few MHz in the frequency range of 2 to 20 GHz.

Using this diagnostic, a search was made for the predicted magnicon output frequency of 11.120 GHz. At the higher magnetic fields (~11 kG) that maximized the deflection cavity gain, only low frequency components (<9.5 GHz) were observed in the output rf pulse. However, as the magnetic field was reduced, the predicted magnicon line appeared in the emission spectrum. At magnetic fields ranging from 6.7–8.2 kG, the dominant spectral feature, and the only spectral peak at frequencies greater than 9.5 GHz, was a strong feature at 11.120 GHz. The spectral feature at 11.120 GHz was present on every shot, responded appropriately to variations of the local oscillator frequency, and also vanished if the microwave signal (before mixing) was filtered using f<8 GHz or f>12 GHz filters. These tests demonstrated that the frequency was correctly identified. An evaluation of the signals from the deflection cavities demonstrated that most of the gain in the experiment was occurring between the third and fourth cavities, and that the fourth cavity was operating very close to instability.

Figure 2 shows a complete set of experimental traces corresponding to conditions under which high power emission at 11.120 GHz was observed. The magnetic field for this shot was 7.9 kG. The magnetron was tuned to 5.560 GHz, and was discharged into the first cavity in advance of the voltage pulse. On this shot, the diode voltage waveform was terminated after the voltage flat-top using the divertor switch in the Marx generator, in order to avoid the cavity oscillations that often occur during the falling portion of the voltage waveform. The first cavity signal corresponds to ~400 W, the second cavity signal to ~500 W, and the third cavity signal to ~2 kW. On this shot, cavities 2 and 3 are demonstrating the gain saturation mechanism described previously. Nevertheless, the penultimate cavity signal reaches ~680 kW in a narrow gain spike, before breaking down. The result is a large signal from cavity 5 (the output cavity), where the pickup is in the far field of the output window.

In order to characterize the output cavity emission, a far–field measurement setup was constructed. In order to ensure that only the 11.120 GHz frequency component would be measured during mode scans, K_u–band waveguide–to–coax adapters, with a 9.5 GHz cutoff

frequency, were used as the microwave pickups. Two pickups, one stationary, and one that swept in the horizontal plane on an 81.3–cm–radius arc about the center of the 3.5–cm output window, were used to measure the radiation antenna pattern. An anechoic enclosure was built around the pickups and the output window. The results for the E_θ and E_r scans are shown in Fig. 3. Each plotted point in Fig. 3 is the average of three experimental shots, and the value from each shot is normalized by the power measured at the stationary pickup. (The data only extends from –75° to +40°, because the stationary pickup was positioned at +50°.) Fig. 3 also shows the calculated far–field radiation pattern for the TE_{21} mode, with the height of the E_θ curve normalized to the peak of the experimental data. The calculation is carried out assuming the presence of a rotating, or circularly-polarized mode, since the scanning-beam interaction in the output cavity should couple to a single circular polarization. The data is clearly in good agreement with the calculated mode pattern.

Using the experimental data in Fig. 3, one can relate the power received by a K_u–band pickup at the angular peak of the pattern to the total power radiated from the output window into 2π. (It is assumed that the scanned horizontal radius is typical.) The method of calculating the power on each shot is illustrated in Table II. The best measured power varied somewhat from day to day (as is typical of many pulsed power experiments). The largest measured signals at the peak of the antenna pattern were in the range of 16.0±0.5 dBm at a magnetic field of 7.2 kG. Summing all of the loss factors, this corresponds to a total radiated power of ~101.4 dBm, or 14 MW, as shown in Table II, corresponding to an efficiency of ~10%. The overall error bar is estimated to be ±3 dB.

Table II. Total Radiated Power Calculation

16.0 ± 0.5 dBm	Peak detected signals (E_θ)
+ 39.7 ± 0.5 dB	Calibrated coax attenuation factor
+ 45.2 ± 0.1 dB	Geometric area factor
− 3.7 ± 3 dB	Ratio of average to peak of antenna pattern
+ 2.5 ± 0.25 dB	Power in E_r Polarization
+ 1.0 ± 0.2 dB	Calibrated pickup loss
+ 0.7 ± 0.2 dB	Effective aperture correction
101.4 ± 3 dBm	Total power (14 MW)

Next, a scan of output power versus magnetic field was made with one pickup at the angular maximum of the antenna pattern. The results are shown in Fig. 4, along with predictions from simulations, as discussed below. The power is seen to peak experimentally at ~8 MW in the vicinity of 7.3 kG, and to vanish both below 6.5 kG and above 8.5 kG. The reason for the loss of high power emission at lower magnetic fields is easily understood. It is observed that high power emission only occurs when there is a large rf signal in the penultimate cavity. This large rf signal becomes erratic below 7 kG, and vanishes completely (during the voltage flat-top) below 6.5 kG. However, the loss of the magnicon signal at higher magnetic fields calls for a different explanation.

It is observed that the large penultimate cavity signal persists at all higher values of magnetic field (through 11 kG), and should provide the required transverse beam momentum to drive the output cavity interaction. In order to examine the predicted behavior of the output cavity as a function of magnetic field, a set of time–dependent simulations of the output cavity were carried out, assuming a constant value of α=0.5, and θ_{sc0}=90°, where θ_{sc0} is the scanning angle spread [7]. (Scanning angle spread is defined as the instantaneous angular extent of the guiding

centers of the electrons in the beam, as viewed from the axis of the cavity.) This value of α was chosen to yield approximately the same peak power as the experimental value, with the scanning angle spread corresponding to the initial beam diameter. These output cavity simulation results are shown in Fig. 4. It is noteworthy that these output cavity simulations predict high power output over a much broader range of magnetic fields (P>2 MW for 6.5<B_z<11 kG) than is observed in the experiment.

In order to understand the parametric dependence of the output power on magnetic field, and the discrepancy between experiment and output cavity simulations, the INP magnicon code (see [6] and references therein) was used to determine the effect of operating the experiment in a situation in which most of the beam spin-up occurs in the penultimate cavity. The magnicon code predicts that the penultimate cavity will be unstable over a broad range of magnetic fields, and can reach high power without being driven by the first cavity. This simulation result is not in complete agreement with the experimental data, which indicate that, over the magnetic field range for which 11.120 GHz emission is observed from the output cavity, a signal from the driver magnetron is generally required in the first cavity in order to induce large rf fields in the penultimate cavity during the voltage flat-top. The penultimate cavity traces from the experiment indicate that the fields build up rapidly when the first cavity is driven, and then suffer an rf breakdown. Based on a calibration of the fourth cavity pickup, the maximum observed fields in the fourth cavity correspond to rf powers of 500 kW to 1 MW, based on the measured cold cavity Q of ~8000. This indicates that the maximum H–fields in the cavity are in the range of 50 to 60 kA/m. The magnicon code predicts that fields this large can result from self-excitation (instability) of the penultimate cavity at magnetic fields above 7.2 kG. Below this magnetic field, the code indicates that some prior beam excitation from cavities 1–3 is needed to drive the penultimate cavity to this level of rf fields.

In addition to experimental data, Figure 4 plots the results from magnicon code simulations. At each magnetic field, the output power is optimized as a function of penultimate

cavity field. These simulations are in good agreement with the experimental results, and predict the rapid fall-off in output power as the magnetic field is increased above 7.5 kG. The highest power simulation point at 6.95 kG, which is somewhat above the highest powers measured in this particular scan, in fact agrees well with the best measured powers that were discussed previously. Experimental operation was observed to become increasingly erratic below 7.2 kG, as the lower gain frequently reduced the magnitude of the penultimate cavity signal. The lack of high power operation below 6.5 kG is also consistent with the simulations, since this corresponds to conditions under which the self-consistent penultimate cavity rf fields are too low to drive high power emission in the absence of large fields in the gain cavities. The most recent experimental results, and the related simulation results, are discussed in detail in [5] which is included as Appendix I.

In summary, short (~50–200 nsec) high power pulses are observed in the deflection cavities, generally followed by rapid rf breakdown. Under the right combination of experimental parameters (650 kV, 225 A, 6.7–8.2 kG magnetic field), a large amplified signal is observed in the penultimate cavity at 5.560 GHz. The amplitude and duration of this signal are limited by rf breakdown. Synchronous with the penultimate cavity signal, a ~100 nsec FWHM frequency–doubled output pulse is observed at 11.120 GHz, twice the measured 5.560 GHz frequency of the penultimate cavity signal. This indicates excitation of the synchronous magnicon mode. A scan of the far–field antenna pattern confirmed that the output power is in the predicted TE_{21} mode (with the output cavity operating in the TM_{210} mode). Based on absolute calibration of the detected microwave signals, the best shots correspond to 14 MW $\pm$ 3 dB at an efficiency of ~10%.

The experimental results demonstrate that the output cavity is driven by the penultimate cavity. The presence of a large penultimate cavity signal during the voltage flat-top is a prerequisite for high power operation of the output cavity. In addition, the shot-to-shot variation in the timing of the penultimate cavity signal is tracked by the timing of the output cavity signal. This evidence suggests that the magnicon may be operating as an amplifier, since, at the optimum magnetic fields

(~7.2 kG), the penultimate cavity signal is only present (during the voltage maximum) if the 5.560 GHz drive signal is present in the first deflection cavity. However, the present operating regime is clearly very close to instability (and is unstable in the simulations), with most of the gain occurring in the penultimate cavity as part of a rapid ramp to high power that is typically terminated by rf breakdown of the penultimate cavity. Furthermore, we have not yet determined the required drive power to produce the output cavity signal, the bandwidth of the interaction, or the degree to which the output signal is frequency or phase locked to the drive signal. All of these must be determined, if amplifier operation is to be confirmed. We have also not found a feasible means to eliminate the plasma effect in the present experiment, in order to operate in a regime of stable penultimate cavity gain.

Work is in progress to further characterize and optimize the operation of the present magnicon experiment. However, it seems evident that the NRL program must transition to a thermionic diode, a cw magnet, a rep–rated modulator (to allow rf conditioning), and an ultrahigh vacuum environment in order to demonstrate the feasibility of efficient, long–pulse, high–duty–factor magnicon amplifiers at 11.4 GHz for linear accelerator applications.

IV. Plans for a Thermionic Magnicon Experiment

The major goal of this programis to design, build, and test a thermionic magnicon amplifier at 11.4 GHz. The key to such an experment is the acquisition of a special high convergence electron gun, since achieving high efficiency operation of a magnicon at 11.4 GHz requires an initial electron beam diameter of no more than ~2 mm. The INP magnicon program makes use of a high convergence electron gun that can produce a 3-mm-diameter electron beam. The chief obstacle to carrying out a thermionic magnicon experiment at NRL has been the acquisition cost of a high power thermionic electron gun to produce the required 100 MW, 2-mm-diameter electron beam. In the absence of sufficient resources to directly purchase such an electron gun, the present strategy is to carry out a collaboration with the Omega-P Corporation, which plans to purchase a Litton electron gun as part of a proposed Phase II Small Business Innovation Research (SBIR) grant from the Department of Energy. The collaboration will also include the redesign of the entire magnicon circuit, in collaboration with Drs. Nezhevenko and Yakovlev of the Budker Institute, who will participate in the collaboration as Omega-P employees. Under a Phase I SBIR grant from DoE, Omega-P has already carried out a preliminary redesign of the 11.4 GHz magnicon circuit. The redesign results in higher efficiency (~58%), lower rf fields, and an improved design for the penultimate and output cavities. As part of the SBIR, Dr. Richard True of Litton Systems, Inc. has carried out a preliminary design of a proposed thermionic electron gun to drive the new magnicon circuit. The properties of the proposed electron gun are shown in Table III. The gun will be fabricated, a new tube designed and built, and a thermionic magnicon experiment carried out over the remaining two years of this program, provided that the Phase II SBIR proposal is funded.

Table III. Properties of Proposed Litton Magnicon Gun

Beam voltage	500 kV
Beam current	200 A
Pulse length	1 μsec
Repetition rate	10 Hz
Final beam diameter	2 mm

V. Magnicon Theory and Simulation

The recent theoretical work has concentrated on the output cavity interaction, and is summarized in three recent papers [7–9]. The paper "Optimization Studies of Magnicon Efficiency," by B. Hafizi and S.H. Gold, presents a study of the effects of beam spreads on out put efficiency using a time-dependent simulation code. This paper is included as Appendix II. The paper "Theory of Competition between Synchronous and Nonsynchronous Modes in a Magnicon Output Cavity," by A.W. Fliflet and S.H. Gold, presents the first analysis of mode competition in the output cavity. Specifically, it studied the competition between the synchronous magnicon mode and nonsynchronous gyrotron modes with stronger coupling to the electron beam. It was found that the magnicon mode supressed the gyrotron modes, provided that the beam spreads were not too large. This paper is included as Appendix III. The paper "Mode Competition in Fourth–Harmonic Magnicon Amplifiers," by A.W. Fliflet and S.H. Gold, studied the design of frequency quadrupling magnicon amplifiers, and evaluated the effects of spreads and of mode competition. It was found that both spreads and mode competition were more serious problems than in second harmonic designs, but that for a high quality electron beam, the competing gyrotron modes were suppressed by the synchronous magnicon mode. This paper is included as Appendix IV.

VI. References

1. M. Karliner, E.V. Kozyrev, I.G. Makarov, O.A. Nezhevenko, G.N. Ostreiko, B.Z. Persov, and G.V. Serdobintsev, "The Magnicon—An Advanced Version of the Gyrocon," *Nucl. Instrum. Methods Phys. Res.*, vol. A269, pp. 459–473, 1988.
2. O.A. Nezhevenko, "Gyrocons and Magnicons: Microwave Generators with Circular Deflection of the Electron Beam," *IEEE Trans. Plasma Sci.*, vol. 22, pp. 765–772, October 1994
3. W.M. Manheimer, "Theory and Conceptual Design of a High–Power Highly Efficient Magnicon at 10 and 20 GHz," *IEEE Trans. Plasma Sci.*, vol. 18, pp. 632–645, 1990.
4. G.I. Budker, M.M. Karliner, I.G. Makarov, S.N. Morosov, O.A. Nezhevenko, G.N. Ostreiko, and I.A. Shekhtman, "The Gyrocon—An Efficient Relativistic High–Power VHF Generator," *Part. Accel.*, vol. 10, pp. 41–59, 1979.
5. S.H. Gold, A.K. Kinkead, A.W. Fliflet, B. Hafizi, and W.M. Manheimer, "Initial Operation of a High Power, Frequency–Doubling X–Band Magnicon Amplifier," *IEEE Trans. Plasma Sci.*, in press.
6. O.A. Nezhevenko, V.P. Yakovlev, S.H. Gold, and B. Hafizi, "Design of a High Power X–Band Magnicon Amplifier," *IEEE Trans. Plasma Sci.*, vol. 22, pp. 785–795, October 1994.
7. A.W. Fliflet and S.H. Gold, "Theory of Competition between Synchronous and Nonsynchronous Modes in a Magnicon Output Cavity," *Phys. Plasmas*, vol. 2, pp. 1760–1765, May 1995.
8. B. Hafizi and S.H. Gold, "Optimization Studies of Magnicon Efficiency," *Phys. Plasmas*, vol. 2, pp. 902–914, March 1995.
9. Arne W. Fliflet and Steven H. Gold, "Mode Competition in Fourth–Harmonic Magnicon Amplifiers," *IEEE Trans. Plasma Sci.*, in press.

VII. Figures

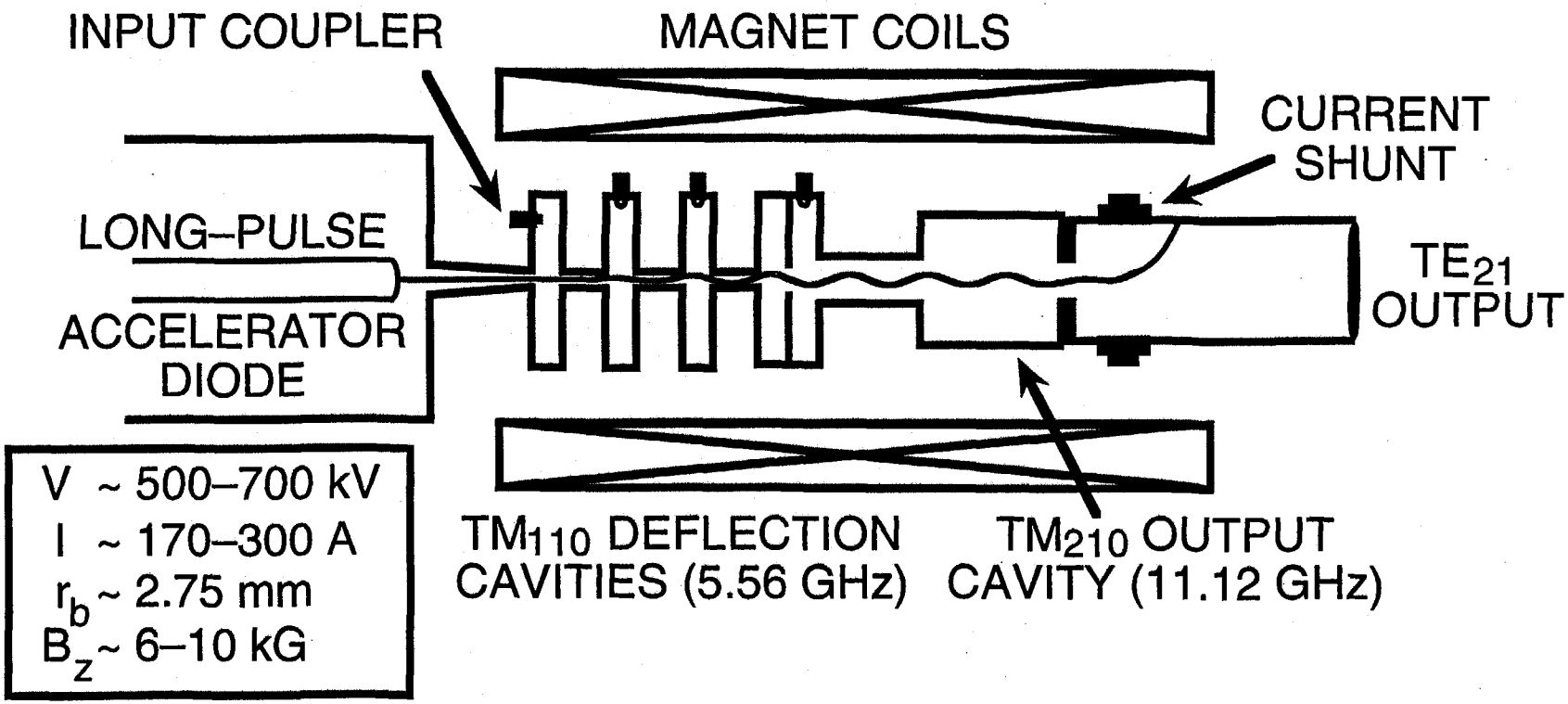

Figure 1. Schematic design of the NRL X–band frequency–doubling magnicon amplifier

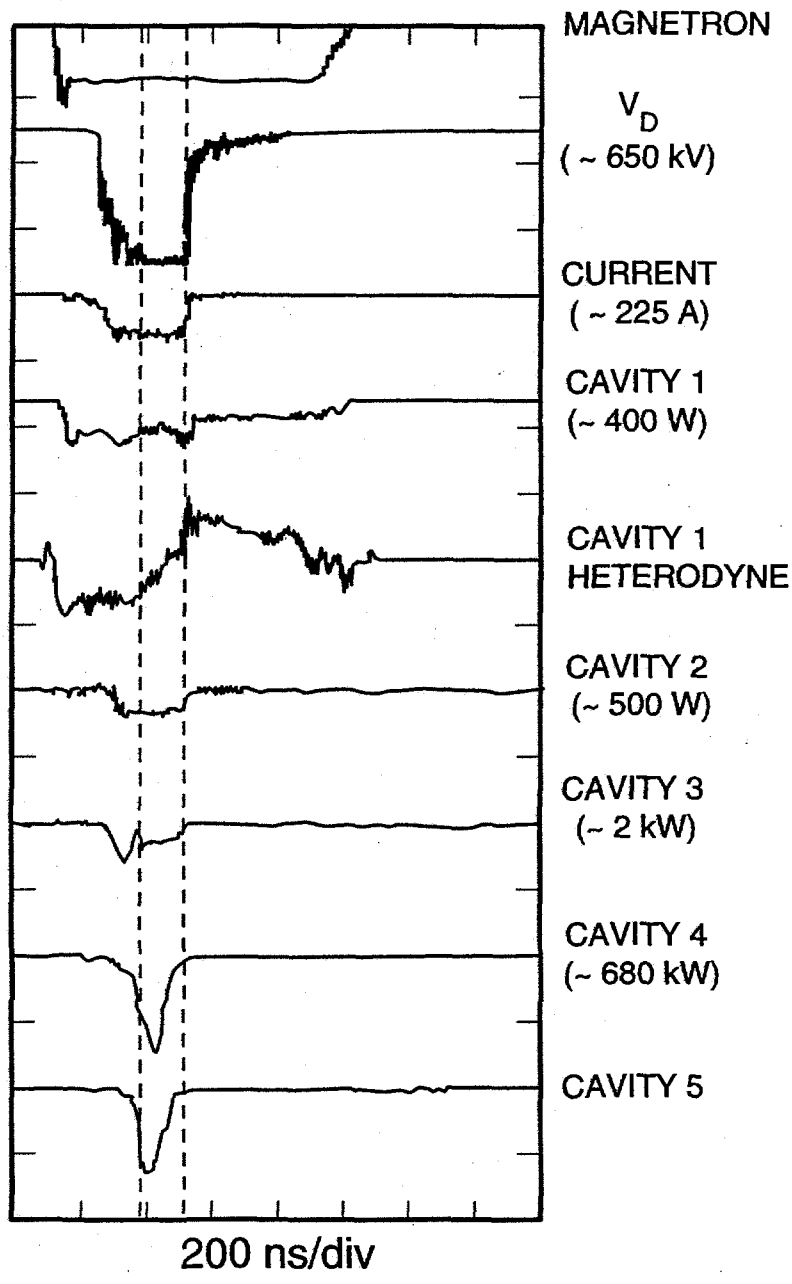

Figure 2. Oscilloscope traces corresponding to magnicon operation at 650 kV, 7.9 kG.

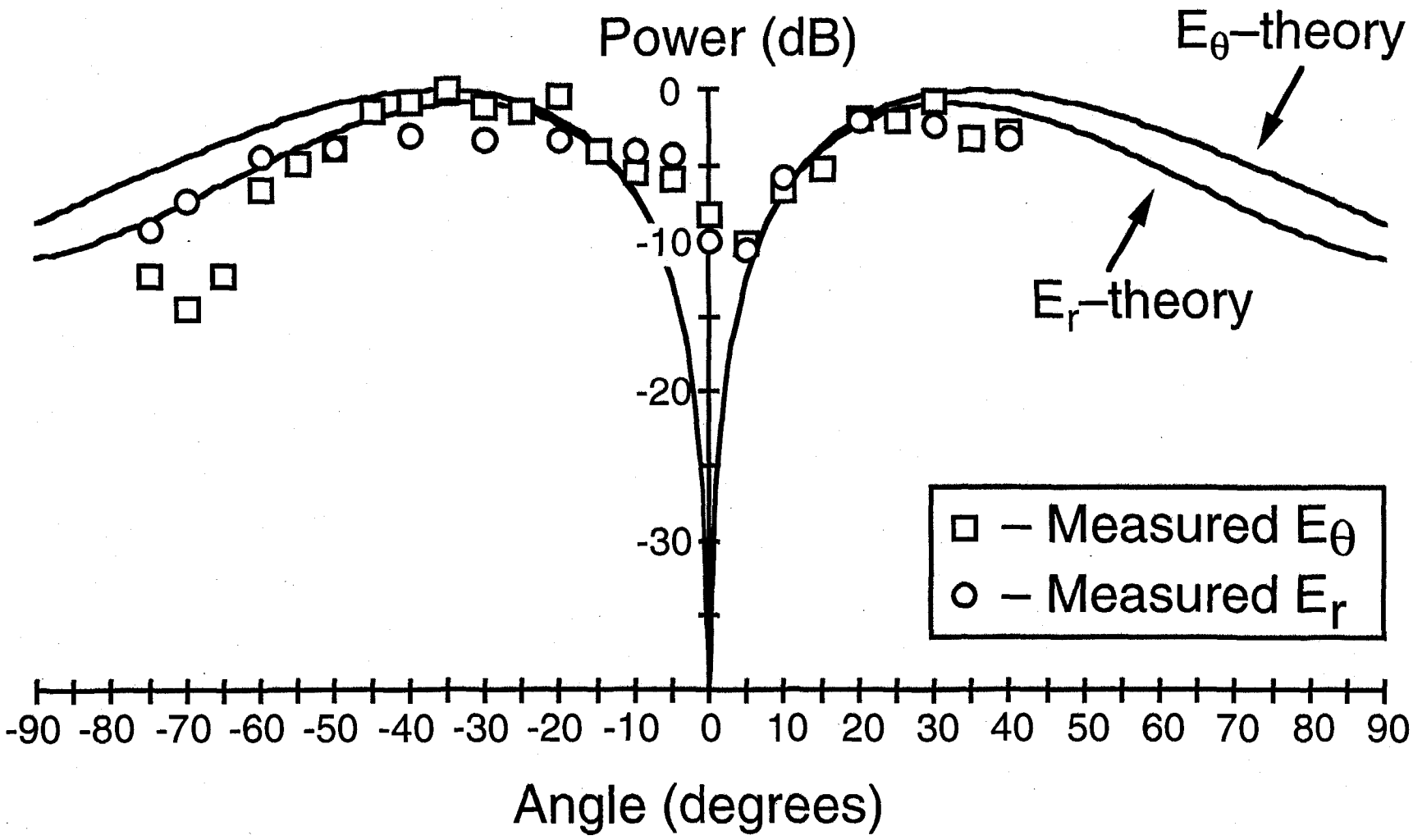

Figure 3. Measured far–field antenna pattern from 3.5–cm–diam. output compared to predictions of theory for the TE_{21} mode.

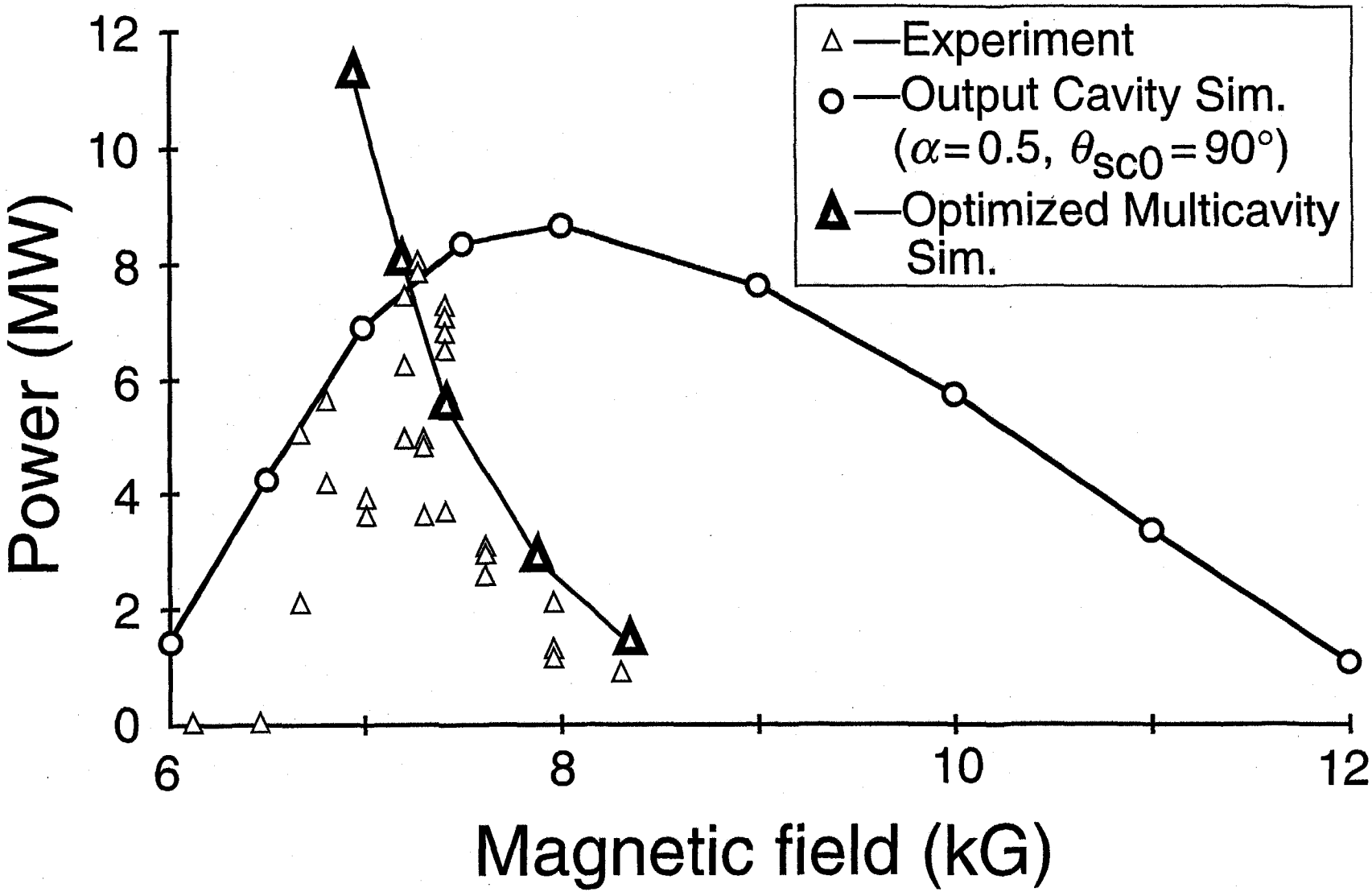

Figure 4. Measured output power versus magnetic field, compared with predictions of theory. Small triangles are data from single experimental shots. Circles are results from a time–dependent output cavity simulation assuming α=0.5 and θ_{sc0}=90°. Large triangles are the results from an optimized multicavity steady–state magnicon simulation.

VIII. Appendices

Appendix I "Initial Operation of a High Power, Frequency–Doubling X–Band Magnicon Amplifier," by S.H. Gold, A.K. Kinkead, A.W. Fliflet, B. Hafizi, and W.M. Manheimer, *IEEE Trans. Plasma Sci.*, in press.

Appendix II "Optimization Studies of Magnicon Efficiency," by B. Hafizi and S.H. Gold, *Phys. Plasmas*, vol. 2, pp. 902–914, March 1995.

Appendix III "Theory of Competition between Synchronous and Nonsynchronous Modes in a Magnicon Output Cavity," by A.W. Fliflet and S.H. Gold, *Phys. Plasmas*, vol. 2, pp. 1760–1765, May 1995.

Appendix IV "Mode Competition in Fourth–Harmonic Magnicon Amplifiers," by Arne W. Fliflet and Steven H. Gold, *IEEE Trans. Plasma Sci.*, in press.

preprint & reprints removed
HH